

## Optical properties and electronic structure of methylammonium iodocuprate as an X-ray scintillator

Andrey A. Petrov,<sup>a</sup> Sergey A. Fateev,<sup>a</sup> Aleksei Yu. Grishko,<sup>a</sup> Artem A. Ordinarov,<sup>a</sup> Andrey V. Petrov,<sup>b</sup> Alexey Yu. Seregin,<sup>c</sup> Pavel V. Dorovatovskii,<sup>c</sup> Eugene A. Goodilin<sup>a,d,e</sup> and Alexey B. Tarasov<sup>\*a,d</sup>

<sup>a</sup> Department of Materials Science, M. V. Lomonosov Moscow State University, 119991 Moscow, Russian Federation. E-mail: alexey.bor.tarasov@yandex.ru

<sup>b</sup> Institute of Chemistry, St. Petersburg State University, 198504 St. Petersburg, Russian Federation

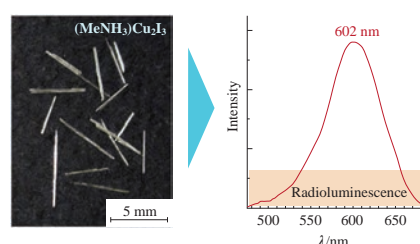
<sup>c</sup> National Research Center 'Kurchatov Institute', 123182 Moscow, Russian Federation

<sup>d</sup> Department of Chemistry, M. V. Lomonosov Moscow State University, 119991 Moscow, Russian Federation

<sup>e</sup> N. S. Kurnakov Institute of General and Inorganic Chemistry, Russian Academy of Sciences, 119991 Moscow, Russian Federation

DOI: 10.1016/j.mencom.2021.01.003

The optical and radioluminescent properties as well as the electronic structure of the recently discovered phase  $(\text{MeNH}_3)\text{Cu}_2\text{I}_3$  are reported for the first time. Single crystals of  $(\text{MeNH}_3)\text{Cu}_2\text{I}_3$  were obtained by crystallization from solution and demonstrated photoluminescence and radioluminescence at 100 K. DFT analysis of both the electronic structure and the partial density of states revealed that  $(\text{MeNH}_3)\text{Cu}_2\text{I}_3$  has a direct bandgap.



**Keywords:** hybrid halide, iodocuprate, X-ray luminescence, radioluminescence, scintillator, DFT, electronic structure.

Organic-inorganic hybrid compounds demonstrate a number of outstanding optoelectronic properties, including photoluminescence, electroluminescence, thermochromic and nonlinear optical properties.<sup>1–3</sup> The incredible success of lead halide perovskites in the last decade gave birth to a new direction in photovoltaics and optoelectronics,<sup>4–7</sup> while attempts to replace lead in the structure with non-toxic metals have contributed to the progress in the synthesis and investigation of other hybrid compounds for optoelectronic applications.<sup>8–10</sup> As a result, dozens of new lead-free hybrid compounds with promising optoelectronic properties have recently been discovered.<sup>11,12</sup> While Bi and Sb-based hybrid halides have been extensively explored in the last five years,<sup>13–20</sup> hybrid halocuprates are still poorly understood.

Halocuprates(I) of organic cations are natural low-dimensional semiconductors that exhibit bright luminescence and phosphorescence,<sup>21–23</sup> as well as thermochromic and photochromic properties.<sup>24</sup> At the same time, it was found that halocuprates of large inorganic cations such as  $\text{Rb}_2\text{CuCl}_3$ ,  $\text{CsCu}_2\text{I}_3$  and  $\text{Cs}_3\text{Cu}_2\text{I}_5$  demonstrate outstanding luminescence intensity. In particular, single crystals of  $\text{Rb}_2\text{CuCl}_3$  were reported,<sup>25</sup> giving a photoluminescence quantum yield of 99.4%, and they were proposed as an X-ray scintillator without self-absorption, showing a light yield of 16600 photons per megaelectronvolt and a large linear scintillation response in the range from  $48.6 \text{ nGy}_{\text{air}} \text{ s}^{-1}$  to  $15.7 \text{ } \mu\text{Gy}_{\text{air}} \text{ s}^{-1}$ .

The  $\text{CsCu}_2\text{I}_3$  phase demonstrated high-intensity photoluminescence attributed to self-trapped excitons<sup>26,27</sup> and was used to make high-speed UV and UV-VIS broadband photodetectors.<sup>28,29</sup> Another cesium iodocuprate,  $\text{Cs}_3\text{Cu}_2\text{I}_5$ , has also been successfully applied to create not only a broadband photodetector<sup>30</sup> but also a deep-blue LED.<sup>31</sup> While many theoretical and experimental studies on the optical

properties and electronic structure of cesium copper halide  $\text{CsCu}_2\text{I}_3$  have been published lately,<sup>26–29,32–38</sup> the optoelectronic properties of the recently reported<sup>39</sup> hybrid copper halide  $(\text{MeNH}_3)\text{Cu}_2\text{I}_3$  have not yet been investigated. Here, we discuss the optical properties of  $(\text{MeNH}_3)\text{Cu}_2\text{I}_3$ , report on its radioluminescence and analyze its electronic structure.

Single crystals of  $(\text{MeNH}_3)\text{Cu}_2\text{I}_3$  [Figure 1(a)] were obtained from a 0.7 M acetonitrile solution by slow evaporation of the solvent in an inert atmosphere to avoid oxidation of  $\text{I}^-$  to  $\text{I}^0$ . It was confirmed that the crystals are composed of  $(\text{MeNH}_3)\text{Cu}_2\text{I}_3$  which crystallizes<sup>†</sup> in the monoclinic space group  $P2_1/m$  with unit cell parameters  $a = 8.9069(1)$ ,  $b = 5.9605(1)$  and  $c = 9.1012(2)$  Å,  $\alpha = 90^\circ$ ,  $\beta = 112.51^\circ$  and  $\gamma = 90^\circ$  in agreement with the known structure<sup>39</sup> [Figures 1(b),(c)].

The diffuse reflectance spectrum<sup>‡</sup> of the powdered crystals of  $(\text{MeNH}_3)\text{Cu}_2\text{I}_3$  in Tauc coordinates [Figure 1(d)] exhibits a steep absorption edge at 3.62 eV, which is close to that obtained from the Tauc plot for  $\text{CsCu}_2\text{I}_3$  (3.77 eV).<sup>33,36</sup> In the UV absorption region, three maxima are observed at 325, 316 and 301 nm (3.82, 3.92 and 4.12 eV, respectively), which can be of excitonic origin due to the low electronic dimensionality and quantum confinement.

<sup>†</sup> Powder X-ray diffraction (XRD) analysis was performed on a Rigaku D/MAX 2500 diffractometer (Japan) with a rotating copper anode using  $\text{CuK}\alpha$  radiation in the range  $2\theta = 5–60^\circ$  with a step of  $0.02^\circ$ . The obtained single crystals were ground in a mortar, and then the XRD pattern of the powder was measured. The profile analysis was carried out using the Jana 2006 software to refine the unit cell parameters.

<sup>‡</sup> The absorption spectra of the ground crystals were recorded in the diffuse reflectance mode on a Perkin Elmer Lambda 950 UV-VIS spectrophotometer.

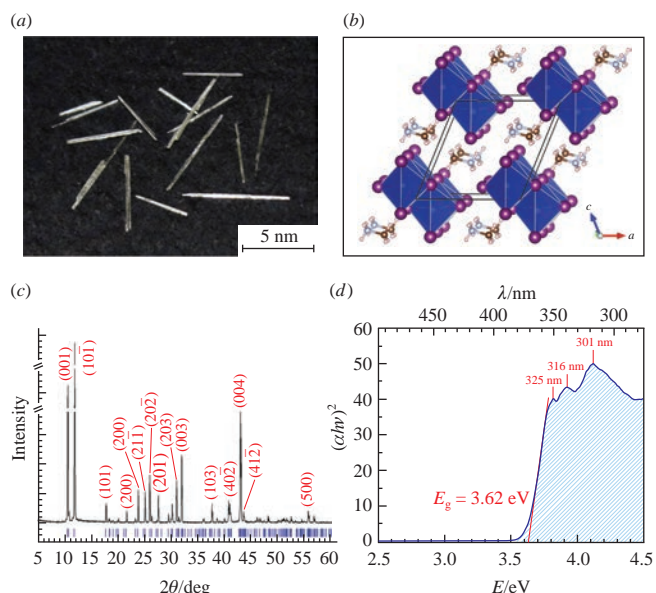


**Figure 1** (a) Single crystals, (b) crystal structure, (c) powder XRD pattern and (d) diffuse reflectance spectrum of  $(\text{MeNH}_3)\text{Cu}_2\text{I}_3$ .

Interestingly, during the X-ray measurement of the  $(\text{MeNH}_3)\text{Cu}_2\text{I}_3$  crystal at the synchrotron radiation source<sup>§</sup> ( $\lambda = 0.9699 \text{ \AA}$ ), the radioluminescence of the sample was observed [Figures 2(a)–(c)]. The glow of a crystal 200  $\mu\text{m}$  in size was so bright that even the naked eye could determine its color as yellowish-orange. Next, we varied the X-ray energy from

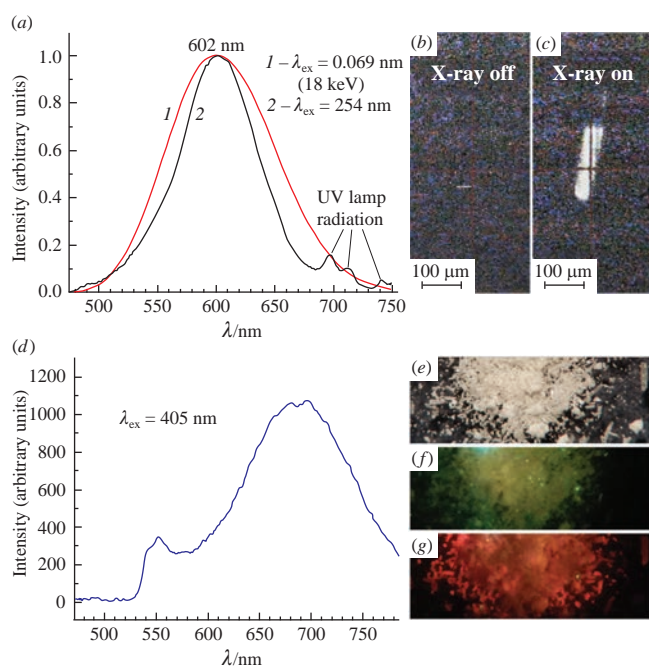
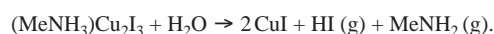


**Figure 2** (a) Spectra of (1) radioluminescence and (2) photoluminescence; (b, c) the appearance of a single crystal of  $(\text{MeNH}_3)\text{Cu}_2\text{I}_3$  (b) without and (c) with X-ray irradiation; (d) photoluminescence spectrum and (e, f, g) photographs of powdered  $(\text{MeNH}_3)\text{Cu}_2\text{I}_3$  in (e) visible light and UV light at 405 nm (f) before and (g) after treatment with water vapor. Photographs (b) and (c) were taken through a Kapton film to filter out UV radiation.

<sup>§</sup> The experiment was performed at the beamline ‘RKFM’ of the Kurchatov specialized source of synchrotron radiation ‘KISI-Kurchatov’. The crystal was secured with a conductive double-sided carbon tape and exposed at an angle of  $45^\circ$  to the beamline. To maintain a temperature of 100 K during the experiments, a Cryostream cooler was used. The spectra were recorded using an optical fiber connected to a Flame-T-VIS-NIR-ES spectrometer (Ocean Optics).

9 keV (0.138 nm) to 18 keV (0.069 nm) and found that the position of the peak does not depend on the radiation energy, while the luminescence intensity increases with increasing radiation energy from 9 to 18 keV. Whereas the radioluminescent  $\text{Rb}_2\text{CuCl}_3$  and the most cognate compound  $\text{CsCu}_2\text{I}_3$  exhibit intense luminescence, this is not the case for  $(\text{MeNH}_3)\text{Cu}_2\text{I}_3$ . The photoluminescence of the latter was observed only after cooling to  $\sim 100 \text{ K}$  with excitation at 254 nm. The peak position is the same as for the radioluminescence, while the FWHM is larger for radioluminescence. In contrast to the ground single crystals, the  $(\text{MeNH}_3)\text{Cu}_2\text{I}_3$  powder, obtained by rapid crystallization using a rotary evaporator, exhibits faint luminescence at 690 nm at room temperature [Figure 2(d)] with excitation at 405 nm. Interestingly, we found that this broad red luminescence also appears after the treatment of the ground single crystals with water vapor [Figure 2(f)] and, apparently, arises due to CuI formed as a result of the reaction:



This assumption is confirmed by the published data<sup>40</sup> that nanocrystalline CuI gives a bright visible luminescence in the deep red region ( $\lambda_{\text{max}} = 688 \text{ nm}$ ) upon excitation at wavelengths of 254, 365 and 405 nm. The shoulder at 550 nm can correspond to the defect states in  $(\text{MeNH}_3)\text{Cu}_2\text{I}_3$ .

To understand the electronic structure of  $(\text{MeNH}_3)\text{Cu}_2\text{I}_3$ , we performed a theoretical calculation of the band structure using the DFT method based on the published crystallographic data.<sup>39</sup> Electronic properties of  $(\text{MeNH}_3)\text{Cu}_2\text{I}_3$  were studied using the DMol<sup>3</sup> module of the Materials Studio software based on DNP (Double Numerical plus polarization) atomic functions and an all-electron approach.<sup>41,42</sup> The electronic structure, including the density of states (DoS) for  $(\text{MeNH}_3)\text{Cu}_2\text{I}_3$ , was calculated using six different functionals. The band gap varied from 2.75 eV for LDA-PWC to 3.44 eV for HCTH (Table 1). The best agreement of the calculation (3.44 eV) with experimental data (3.62 eV)

**Table 1** Band gap energy of  $(\text{MeNH}_3)\text{Cu}_2\text{I}_3$  calculated using various functionals.

Functional	LDA-PWC	PBE	PW91	BLYP	BOP	HCTH
$\Delta E_g/\text{eV}$	2.75	2.94	3.08	2.97	3.08	3.44

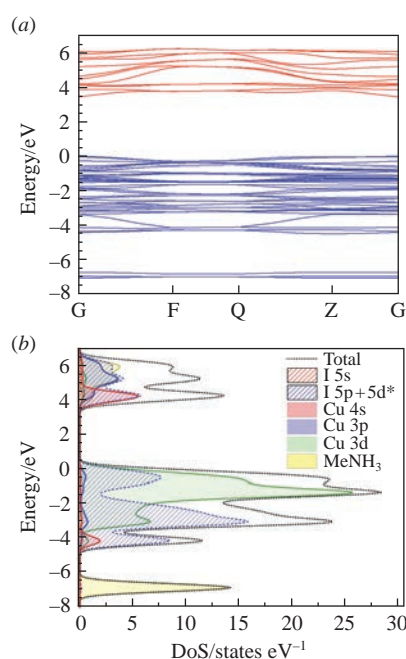


**Figure 3** (a) Band structure and (b) partial density of states of  $(\text{MeNH}_3)\text{Cu}_2\text{I}_3$ .

was found for the HCTH functional. The calculations show that the  $(\text{MeNH}_3)\text{Cu}_2\text{I}_3$  phase is a direct-gap semiconductor with a bandgap at the  $\Gamma$  point [Figure 3(a)]. The density of states indicates [Figure 3(b)] that the VBM consists mainly of Cu 3d and I 5p orbitals, while the CBM consists of Cu 4s and I 5p orbitals, which is the same as for  $\text{CsCu}_2\text{I}_3$ .<sup>29,32</sup> It can be seen that the energy levels of the methylammonium cations lie deep below the valence band and do not contribute to the VBM. However, they also contribute to the conduction band but not to the CBM. Compared to  $\text{CsCu}_2\text{I}_3$ ,  $(\text{MeNH}_3)\text{Cu}_2\text{I}_3$  has a similar dispersion of the VBM, but a more flat CBM indicates a larger electron effective mass.

In summary, a simple procedure is proposed for growing large single crystals of  $(\text{MeNH}_3)\text{Cu}_2\text{I}_3$  from acetonitrile solution. The optical properties and electronic structure of  $(\text{MeNH}_3)\text{Cu}_2\text{I}_3$ , investigated for the first time, reveal the optical band gap of  $(\text{MeNH}_3)\text{Cu}_2\text{I}_3$  equal to 3.62 eV, which is slightly lower than that of the cesium analog  $\text{CsCu}_2\text{I}_3$  (3.77 eV). An analysis of the electronic structure confirmed that  $(\text{MeNH}_3)\text{Cu}_2\text{I}_3$  has a direct band gap, with VBM consisting mainly of Cu 3d and I 5p orbitals, and CBM consisting of Cu 4s and I 5p orbitals.  $(\text{MeNH}_3)\text{Cu}_2\text{I}_3$  has been found to exhibit radioluminescence in the soft X-ray region, which makes it a possible candidate for use in scintillators.

This research was supported by the Russian Foundation for Basic Research (project no. 20-33-70265). We thank colleagues from the Joint Research Center for Physical Methods of Research of IGIC RAS for their valuable assistance in sample analysis. The radioluminescence experiments were performed at the beamline 'RKFM' of the Kurchatov specialized source of synchrotron radiation 'KISI-Kurchatov'. DFT calculations were carried out using computational resources provided by Resource Center 'Computer Center of SPbU' (<http://cc.spbu.ru>).

## References

- 1 Hybrid Materials: Synthesis, Characterization, and Applications, ed. G. Kickelbick, Wiley-VCH, Weinheim, 2007.
- 2 S. Parola, B. Julián-López, L. D. Carlos and C. Sanchez, *Adv. Funct. Mater.*, 2016, **26**, 6506.
- 3 D. B. Mitzi, in *Progress in Inorganic Chemistry*, ed. K. D. Karlin, John Wiley & Sons, New York, 1999, vol. 48, pp. 1–121.
- 4 J.-P. Correa-Baena, A. Abate, M. Saliba, W. Tress, T. J. Jacobsson, M. Grätzel and A. Hagfeldt, *Energy Environ. Sci.*, 2017, **10**, 710.
- 5 P. K. Nayak, S. Mahesh, H. J. Snaith and D. Cahen, *Nat. Rev. Mater.*, 2019, **4**, 269.
- 6 M. V. Kovalenko, L. Protesescu and M. I. Bodnarchuk, *Science*, 2017, **358**, 745.
- 7 N. Belich, N. Udalova, A. Semenova, A. Petrov, S. Fateev, A. Tarasov and E. Goodilin, *Front. Chem.*, 2020, **8**, 550625.
- 8 Y. Chen, Y. Sun, J. Peng, J. Tang, K. Zheng and Z. Liang, *Adv. Mater.*, 2018, **30**, 1703487.
- 9 S. F. Hoefler, G. Trimmel and T. Rath, *Monatsh. Chem.*, 2017, **148**, 795.
- 10 T. Miyasaka, A. Kulkarni, G. M. Kim, S. Öz and A. K. Jena, *Adv. Energy Mater.*, 2020, **10**, 1902500.
- 11 E. I. Marchenko, S. A. Fateev, A. A. Petrov, E. A. Goodilin and A. B. Tarasov, *Mendeleev Commun.*, 2020, **30**, 279.
- 12 E. I. Marchenko, S. A. Fateev, A. A. Petrov, V. V. Korolev, A. Mitrofanov, A. V. Petrov, E. A. Goodilin and A. B. Tarasov, *Chem. Mater.*, 2020, **32**, 7383.
- 13 S. A. Adonin, M. N. Sokolov and V. P. Fedin, *Russ. J. Inorg. Chem.*, 2017, **62**, 1789.
- 14 S. A. Adonin, L. A. Frolova, M. N. Sokolov, G. V. Shilov, D. V. Korchagin, V. P. Fedin, S. M. Aldoshin, K. J. Stevenson and P. A. Troshin, *Adv. Energy Mater.*, 2018, **8**, 1701140.
- 15 N. A. Yelovik, A. V. Mironov, M. A. Bykov, A. N. Kuznetsov, A. V. Grigorieva, Z. Wei, E. V. Dikarev and A. V. Shevelkov, *Inorg. Chem.*, 2016, **55**, 4132.
- 16 T. A. Shestimerova, A. V. Mironov, M. A. Bykov, A. V. Grigorieva, Z. Wei, E. V. Dikarev and A. V. Shevelkov, *Molecules*, 2020, **25**, 2765.
- 17 S. A. Adonin, I. D. Gorokh, A. S. Novikov, D. G. Samsonenko, I. V. Yushina, M. N. Sokolov and V. P. Fedin, *CrystEngComm*, 2018, **20**, 7766.
- 18 V. Morad, S. Yakunin and M. V. Kovalenko, *ACS Mater. Lett.*, 2020, **2**, 845.
- 19 S. A. Adonin, I. D. Gorokh, P. A. Abramov, I. V. Korolkov, M. N. Sokolov and V. P. Fedin, *Mendeleev Commun.*, 2018, **28**, 39.
- 20 S. A. Adonin, I. D. Gorokh, A. S. Novikov, A. N. Usoltsev, M. N. Sokolov and V. P. Fedin, *Inorg. Chem. Commun.*, 2019, **103**, 72.
- 21 S. Chen, J. Gao, J. Chang, Y. Li, C. Huangfu, H. Meng, Y. Wang, G. Xia and L. Feng, *ACS Appl. Mater. Interfaces*, 2019, **11**, 17513.
- 22 W. Liu, Y. Fang and J. Li, *Adv. Funct. Mater.*, 2018, **28**, 1705593.
- 23 W. Liu, K. Zhu, S. J. Teat, G. Dey, Z. Shen, L. Wang, D. M. O'Carroll and J. Li, *J. Am. Chem. Soc.*, 2017, **139**, 9281.
- 24 J.-J. Shen, X.-X. Li, T.-L. Yu, F. Wang, P.-F. Hao and Y.-L. Fu, *Inorg. Chem.*, 2016, **55**, 8271.
- 25 X. Zhao, G. Niu, J. Zhu, B. Yang, J.-H. Yuan, S. Li, W. Gao, Q. Hu, L. Yin, K.-H. Xue, E. Lifshitz, X. Miao and J. Tang, *J. Phys. Chem. Lett.*, 2020, **11**, 1873.
- 26 R. Roccanova, A. Yangui, G. Seo, T. D. Creason, Y. Wu, D. Y. Kim, M.-H. Du and B. Saparov, *ACS Mater. Lett.*, 2019, **1**, 459.
- 27 R. Lin, Q. Zhu, Q. Guo, Y. Zhu, W. Zheng and F. Huang, *J. Phys. Chem. C*, 2020, **124**, 20469.
- 28 Z. Li, Z. Li, Z. Shi and X. Fang, *Adv. Funct. Mater.*, 2020, **30**, 2002634.
- 29 J. Yang, W. Kang, Z. Liu, M. Pi, L.-B. Luo, C. Li, H. Lin, Z. Luo, J. Du, M. Zhou and X. Tang, *J. Phys. Chem. Lett.*, 2020, **11**, 6880.
- 30 W. Liang, Z. Shi, Y. Li, J. Ma, S. Yin, X. Chen, D. Wu, Y. Tian, Y. Zhang, X. Li and C. Shan, *ACS Appl. Mater. Interfaces*, 2020, **12**, 37363.
- 31 L. Wang, Z. Shi, Z. Ma, D. Yang, F. Zhang, X. Ji, M. Wang, X. Chen, G. Na, S. Chen, D. Wu, Y. Zhang, X. Li, L. Zhang and C. Shan, *Nano Lett.*, 2020, **20**, 3568.
- 32 T. Jun, T. Handa, K. Sim, S. Iimura, M. Sasase, J. Kim, Y. Kanemitsu and H. Hosono, *APL Mater.*, 2019, **7**, 111113.
- 33 R. Kentsch, M. Morgenroth, M. Scholz, K. Xu, J. Schmedt auf der Günne, T. Lenzer and K. Oum, *J. Phys. Chem. Lett.*, 2020, **11**, 4286.
- 34 Q. Li, Z. Chen, B. Yang, L. Tan, B. Xu, J. Han, Y. Zhao, J. Tang and Z. Quan, *J. Am. Chem. Soc.*, 2020, **142**, 1786.
- 35 M.-H. Du, *ACS Energy Lett.*, 2020, **5**, 464.
- 36 R. Lin, Q. Guo, Q. Zhu, Y. Zhu, W. Zheng and F. Huang, *Adv. Mater.*, 2019, **31**, 1905079.
- 37 P. Sebastia-Luna, J. Navarro-Alapont, M. Sessolo, F. Palazon and H. J. Bolink, *Chem. Mater.*, 2019, **31**, 10205.
- 38 P. Vashishtha, G. V. Nutan, B. E. Griffith, Y. Fang, D. Giovanni, M. Jagadeeswararao, T. C. Sum, N. Mathews, S. G. Mhaisalkar, J. V. Hanna and T. White, *Chem. Mater.*, 2019, **31**, 9003.
- 39 A. A. Petrov, V. N. Khrustalev, Y. V. Zubavichus, P. V. Dorovatovskii, E. A. Goodilin and A. B. Tarasov, *Mendeleev Commun.*, 2018, **28**, 245.
- 40 S. Saha, S. Das, D. Sen, U. K. Ghorai, N. Mazumder, B. K. Gupta and K. K. Chattopadhyay, *J. Mater. Chem. C*, 2015, **3**, 6786.
- 41 B. Delley, *J. Chem. Phys.*, 1990, **92**, 508.
- 42 B. Delley, *J. Chem. Phys.*, 2000, **113**, 7756.

Received: 9th November 2020; Com. 20/6361